HHS Public Access

Author manuscript

Gene. Author manuscript; available in PMC 2015 March 03.

Published in final edited form as:

Gene. 2004 August 18; 338(1): 25–34. doi:10.1016/j.gene.2004.05.002.

Structural, expression, and evolutionary analysis of mouse *CIAS1*☆,☆☆

Justin P. Anderson[a,1], **James L. Mueller**[a,b,1], **Sanna Rosengren**[c], **David L. Boyle**[c], **Philip Schaner**[d], **Steven B. Cannon**[e], **Carl S. Goodyear**[c], and **Hal M. Hoffman**[a,b,c,*]

[a]Department of Pediatrics, University of California San Diego School of Medicine, La Jolla, CA 92093, USA

[b]Ludwig Institute of Cancer Research, University of California San Diego School of Medicine, La Jolla, CA 92093, USA

[c]UCSD Division of Rheumatology, Allergy, and Immunology, Rheumatic Disease Core Center, University of California San Diego School of Medicine, 9500 Gilman Drive, La Jolla, CA 92093-0635, USA

[d]Department of Cell and Developmental Biology, University of Michigan, Ann Arbor, MI 48109-0616, USA

[e]Department of Plant Pathology, University of Minnesota, St. Paul, MN 55108 USA

Abstract

Mutations in the human *CIAS1* (*hCIAS1*) gene have been identified in a continuum of inflammatory disorders including familial cold autoinflammatory syndrome (FCAS), Muckle–Wells syndrome (MWS), and neonatal onset multisystem inflammatory disease (NOMID). *CIAS1* codes for the protein Cryopyrin, which appears to play a role in innate immune function by regulating the production of proinflammatory cytokines. Human and mouse Cryopyrin are highly conserved and consist of three functional domains including a pyrin domain, an NACHT domain,

---

☆Supplementary data associated with this article can be found, in the online version, at doi: 10.1016/j.gene.2004.05.002.

☆☆The nucleotide sequence data reported in this paper have been submitted to GenBank and have been assigned the accession numbers for the three mouse strains (strain C57BL/6) *CIAS1*.mRNA AY337285– *CIAS1*.Exon1 AY337286, *CIAS1*.Exon2 AY337287, *CIAS1*.Exon3 AY337288, *CIAS1*.Exon4 AY337289, *CIAS1*.Exon5 AY337290, *CIAS1*.Exon6 AY337291, *CIAS1*.Exons7– 9 AY337292, (strain BALB/c) *CIAS1*.mRNA variant 1 AY495376, *CIAS1*.mRNA variant 2 AY495377, *CIAS1*.Exon1 AY337293, *CIAS1*.Exon2 AY337294, *CIAS1*.Exon3 AY337295, *CIAS1*.Exon4 AY337296, *CIAS1*.Exon5 AY337297, *CIAS1*.Exon6 AY337298, *CIAS1*.Exon7–9 AY337299, (strain 129/Sv) *CIAS1*.Exon1 AY337300, *CIAS1*.Exon2 AY337301, *CIAS1*.Exon3 AY337302, *CIAS1*.Exon4 AY337303, *CIAS1*.Exon5 AY337304, *CIAS1*.Exon6 AY337305, *CIAS1*.Exon7– 9 AY337306. The primate sequence accession numbers are Gg*CIAS1*.Exon1 AY337307, Tg*CIAS1*.Exon1 AY337308, Ms*CIAS1*.Exon1 AY337309, Ab*CIAS1*.Exon1 AY337310, Cj*CIAS1*.Exon1 AY337311, Cm*CIAS1*.Exon1 AY337312, Gg*CIAS1*.NBS AY338196, Tg*CIAS1*.NBS AY338197, Ms*CIAS1*.NBS AY338198, Cc*CIAS1*.NBS AY338199, Cg*CIAS1*.NBS AY338200, Ab*CIAS1*.NBS AY338201, Aa*CIAS1*.NBS AY338202, Ss*CIAS1*.NBS AY338203, Ca*CIAS1*.NBS AY338204, S.*CIAS1*.NBS AY338205, Cj*CIAS1*.NBS AY338206, Cp.*CIAS1*.NBS AY338207, Tb*CIAS1*.NBS AY338208, Cm*CIAS1*.NBS AY338209, Lc*CIAS1*.NBS AY338210, and Vv*CIAS1*.NBS AY338211. The mammalian sequence accession numbers are La*CIAS1*.NBS AY495378, Ee*CIAS1*.NBS AY495379, and Dn*CIAS1*.NBS AY495380.

*Corresponding author. UCSD Division of Rheumatology, Allergy, and Immunology, University of California San Diego School of Medicine, 9500 Gilman Drive, La Jolla, CA 92093-0635, USA. Tel.: +1-858-534-2108; fax: +1-858-534-2110. hahoffman@ucsd.edu (H.M. Hoffman).

[1]These authors contributed equally to this work.

and a leucine-rich repeat (LRR) domain that are characteristics of the NALP family of proteins. The pyrin and NACHT domains of Cryopyrin and other NALP proteins are highly conserved among primate and nonprimate mammals, suggesting purifying selection throughout mammalian evolution. Cryopyrin expression is also very similar in human and mouse with mouse *CIAS1* mRNA expression found primarily in peripheral blood leukocytes consistent with the postulated inflammatory function. We also detected significant expression in mouse eye and skin tissue, which is consistent with symptoms observed in human Cryopyrin-associated diseases.

Keywords

Cryopyrin; Pyrin; Primate; NACHT; Autoinflammatory; NALP

1. Introduction

A new family of proteins involved in innate immunity has recently been identified in humans. The common characteristics of proteins in this family are the presence of certain structural domains such as caspase recruitment domains and pyrin domains (PYD). Several of these proteins, referred to as NALP, NOD, or CATERPILLAR proteins, also contain purine nucleotide-binding NACHT domains, and leucine-rich repeat (LRR) domains (Harton et al., 2002; Tschopp et al., 2003). Four of these proteins have been associated with human diseases, including pyrin, NOD2, major histocompatibility complex (MHC) class II transactivator (CIITA), and Cryopyrin. Alterations in pyrin result in familial Mediterranean fever (FMF), a recessively inherited periodic fever disorder characterized by intermittent episodes of fever, arthritis, rash, and abdominal pain (French FMF Consortium, 1997; International FMF Consortium, 1997). Mutations in the gene for CIITA are associated with a rare recessively inherited cellular immune deficiency called bare lymphocyte syndrome, which is characterized by a lack of MHC class II gene expression resulting in susceptibility to infection early in life (Steimle et al., 1993). Mutations in NOD2 have been associated with susceptibility to Crohn's disease, a relatively common inflammatory disease of the gastrointestinal tract (Hugot et al., 2001; Ogura et al., 2001a), and Blau syndrome, a rare dominantly inherited granulomatous disorder involving skin, joints, and eyes (Miceli-Richard et al., 2001). Cryopyrin (also known as NALP3/Pypaf1) is altered in patients with a spectrum of inflammatory syndromes characterized by fever, as well as cutaneous, joint, and neurosensory symptoms (Feldmann et al., 2002; Hoffman et al., 2001a).

CIAS1 mutations are associated with a continuum of phenotypes that encompass three previously recognized syndromes. Familial cold autoinflammatory syndrome (FCAS MIM 120100), commonly known as familial cold urticaria, is an autosomal dominant systemic inflammatory disease characterized by intermittent episodes of rash, arthralgia, fever, and conjunctivitis after generalized exposure to cold (Hoffman et al., 2001b). Patients with Muckle–Wells syndrome (MWS MIM 191900) have similar episodes to those of FCAS, but symptoms are usually not associated with cold exposure. A significant percentage of patients with MWS also develop progressive sensorineural hearing loss (~ 60%) and systemic amyloidosis (~ 30%) leading to renal failure (Muckle, 1979). Neonatal onset multisystem inflammatory disease (NOMID MIM 607115) is primarily sporadic, but dominant

transmission has been documented. These patients have chronic systemic inflammation involving the skin, joints, and central nervous system, and also have cartilage overgrowth, hearing loss, and eye disease (Prieur et al., 1987). There is some correlation of specific *CIAS1* nucleotide substitutions with phenotype; however, the same mutation has been associated with different phenotypes in different patients suggesting additional genetic or environmental influences (Dode et al., 2002; Neven et al., 2004).

Mouse models of human disease can be used to elucidate genetic and immunologic mechanisms in ways not feasible in the human model. Mouse knockout models for CIITA and pyrin, both proteins associated with the recessive disorders discussed above, have provided significant insight into pathophysiology (Chae et al., 2003; Chang et al., 1996). The availability of the mouse genome sequence has made the identification of human disease gene orthologs relatively straightforward (Reed et al., 2003). However, genetic strain variation and tissue and cell expression studies are necessary before the development of a mouse model, because variation between humans and mice at the DNA, RNA expression, or protein level often create significant differences in phenotypic expression. In this paper, we demonstrate that the mouse homolog of *CIAS1* has significant similarities in expression to human *CIAS1* with patterns consistent with clinical symptoms. We also analyze the evolutionary history of *CIAS1* and contrast it to the gene that codes for the related protein pyrin.

2. Materials and methods

2.1. Database search of genome sequence

The National Center for Biotechnology Information (NCBI) and UCSC Genome mouse databases were searched using the Basic Local Alignment Search Tool (BLAST: http://www.ncbi.nlm.nih.gov/BLAST/, and BLAT: http://genome.ucsc.edu/) programs with the human *CIAS1* (*hCIAS1*) ORF (AF410477) and predicted protein sequence (AAL33908) to find the DNA sequences of mouse *CIAS1* (*mCIAS1*) and the 14 known human NALP genes (Table 1). BLAST searches were also performed against the NCBI and Ensembl databases for *D. rerio* (zebrafish), *D. melanogaster* (*Drosophila*), *C. elegans* (nematode), and *Fugu rubripes* (pufferfish) (http://www.ensembl.org/).

2.2. Mouse genomic DNA amplification and sequencing

Mouse-tail preps were used to isolate genomic DNA from the BALB/c and C57BL/6 strains. Embryonic stem cell DNA and RPI22 269L7 and 157J5 BAC clones (Children's Hospital Oakland http://bacpac.chori.org/home.htm) from chromosome 11 (Chr 11) were used for the 129/SV strain. Genomic sequence surrounding *mCIAS1* was used to design *mCIAS1*-specific primers for PCR and sequencing of *mCIAS1*. Primers were designed by using Primer3 (http://www-genome.wi.mit.edu/cgi-bin/primer/primer3_www.cgi). The PCR conditions and primers used to amplify and sequence mouse genomic DNA are shown in Supplementary Table 1.

2.3. Rapid amplification of 5′ and 3′cDNA ends (5′ and 3′ RACE) for the mCIAS1 gene

To amplify and sequence the 5′ and 3′ cDNA ends of *mCIAS1*, we used a mouse spleen Marathon-Ready cDNA kit (Clontech). The RACE reactions were performed according to manufacturer's protocol. The primers used for the 5′ end were Mex-2F (sense: 5′-ACCCAAGGCTGCTATCTGG-3′), *mCIAS1*ex1R (antisense: 5′-TTCTCCTCGCCATTGAAGTC-3′), PyrinckR (Supplementary Table 2), MP1R (antisense: 5′-GCTAGGATGGTTTTCCCGAT-3′), Mx2-mx3R (Supplementary Table 1), and Mex2-3SeqR (Supplementary Table 1). The primers used for the 3′ end were Mx3-mx4aF (sense: 5′-TGAAGTGGATTGAAGTGAAAGC-3′), *mCIAS1*ex8F (Supplementary Table 1), *mCIAS1*3′utrFb (sense: 5′-TTTCTCTCTCTGGGCCTCTG-3′), and *mCIAS1*3′utrR (sense: 5′-GGGTTTTATAAATCTCTGAG-3′). PCR products were then purified, sequenced, and analyzed as previously reported (Kolodner et al., 1999).

2.4. Cloning of the mCIAS1 ORF

The primers MFLFwd (sense: 5′-CTGCTGCTGAAGATGACGAG-3′) and MFLRev (antisense: 5′-GCCTACCAGGAAATCTCGAA-3′) were used to amplify the entire coding sequence of the *mCIAS1* gene from mouse spleen cDNA. The PCR reactions were prepared as described in Supplementary Table 1 with the following conditions: an initial denaturation step of 94 °C for 30 s; followed by five cycles of 94 °C for 5 s and 72 °C for 4 min, five cycles of 94 °C for 5 s and 70 °C for 4 min, and 20 cycles of 94 °C for 5 s and 68 °C for 4 min. The PCR product was directly cloned into pCR®-Blunt II-TOPO® vector (Invitrogen™). The clone was fully sequenced and aligned with genomic sequence to confirm the intron–exon structure and that sequence was identical to the MMIG gene (AF486632) recently reported (Kikuchi-Yanoshita et al., 2003).

2.5. Northern blot analysis of mCIAS1 expression

A PCR product of 599 bp corresponding to nucleotides 96–695 of the *mCIAS1* ORF was amplified from mouse cDNA and gel purified from 1% agarose. This and a β-actin control probe were radioactively labeled with [α^{32}P] dCTP using PrimeIt® II (Stratagene) and purified on a G-25 Sephadex column (Boehringer Mannheim). The probes were hybridized to the Northern blots (Clontech) for 1 h at 68 °C in ExpressHyb™ solution (Clontech), washed at 50–65 °C according to the manufacturer's instructions and analyzed by autoradiography.

2.6. Isolation of mouse tissue and blood

Mouse tissues were collected from C57BL/6, frozen at −80 °C, and then homogenized. Whole blood was obtained by direct heart puncture from BALB/c mice and separated by centrifugation using Lympholyte® (Cedarlane®) according to manufacturer's protocol. The granulocyte fraction was obtained by red blood cell lysis of the lower layer, and peripheral blood mononuclear cells (PBMCs) were collected from the upper layer. PBMCs were further separated using the MACS® murine monocyte positive selection beads (Miltenyi Biotec). Purity of cell populations was confirmed by FACS analysis. Mononuclear cells were stained with FITC-labeled anti-CD3 (clone 145-2C11), APC-labeled anti-CD45R/B200 (clone RA3-6B2) or isotype controls (BD-Pharmingen), PE-labeled F4/80

(cloneCI:A3-1) (Cal-tag) in the presence of Fc block (BD-Pharmingen) as appropriate. Data were acquired using a FACSCalibur™ (BD Biosciences) and analyzed with FlowJo software (Treestar). Forward and side-scatter gates included only nucleated viable cells, dead cells were excluded based on light scatter and 7-AAD uptake. Purity was further confirmed using microscopic analysis of Wright-stained cytospins. The granulocyte cell fraction was greater than 90% pure. PBMCs were 98% pure and were further fractionated into a monocyte fraction with greater than 50% purity (enriched eightfold) and a lymphocyte fraction with 99% purity. Mouse bone marrow-derived mast cells were generated as reported previously (Razin et al., 1981).

2.7. RNA isolation, reverse transcriptase PCR, and quantitative real-time PCR

Total RNA isolation was performed using the TRIzol® Reagent protocol (Invitrogen™). Reverse transcriptase PCR was then performed using SuperScript™ First-Strand Synthesis System (Invitrogen™) using manufacturer's protocols and primers and several *mCIAS1*-specific primers. Quantitative real-time PCR analysis was performed using TaqMan® technology. RNA was reverse-transcribed to yield cDNA using Applied Biosystems reagents. A primer/probe set was designed to anneal at the junction of coding exons 1–2 of *CIAS1* (sense: 5′-TGTGTGGATCTTTGCTGCGA-3′; antisense: 5′-GTCATTCCACTCTGGCTGGTC-3′; probe, 6 FAM - 5 ′-ACAGGCGAGACCTCTGGGAAAAAGCTAAG-3′-TAMRA; all used at 200 nM final concentration). A primer/probe set for the housekeeping gene *HPRT* was obtained from Applied Biosystems (Assay-On-Demand) and used as recommended. For each cDNA, separate PCR reactions were run with *mCIAS1* and *HPRT* reagents in TaqMan® Universal PCR Master Mix (Applied Biosystems). Resulting threshold cycle (C_t) data were normalized to standard curves constructed using serial dilutions of mouse PBMC cDNA yielding cell equivalents. Data are expressed as the ratio between *mCIAS1* and *HPRT* cell equivalents (relative expression units, REU) as described previously (Boyle et al., 2003). Each PCR run also included nontemplate controls, which generated a C_t greater than 40 in all experiments.

2.8. Primate and mammalian ortholog sequencing

The NACHT domain was sequenced for select old world, new world, lower primates, and other mammals. The old world primates sequenced were *G. gorilla* (gorilla), *T. gelada* (baboon), *M. sylvanus* (macaque), *C. cephus* (guenon), and *C. guereza* (colobus). The new world primates sequenced were *A. belzebul* (howler monkey), *A. azarae* (owl monkey), *S. sciureus* (squirrel monkey), *C. apella* (capuchin), *S. midas* (tamarin), *C. jacchus* (common marmoset), and *C. pygmaea* (pygmy marmoset). The NACHT domain was only partially sequenced for the following lower primates and other mammals: *T. bancanus* (tarsier), *C. medius* (dwarf lemur), *L. catta* (ring tailed lemur), *V. variegata* (ruffed lemur), *L. africanus* (African elephant), *E. europaeus* (Western European hedgehog), and *D. novem-cinctus* (nine-banded armadillo).

To sequence the NACHT domain of these mammals, primers were first designed in the most conserved regions found by comparing human and mouse DNA sequences. Human DNA sequence was used for any nonconserved bases. Further primer design was necessary to sequence the lower primates and mammals. As we sequenced more animals, those

sequences were used in creating new primers in the most conserved regions. The PYD was only sequenced for a few of the primates due to difficulty with the amplification of this region. Primers were used first from human DNA sequence, and then from primate sequence once it was obtained. The PCR conditions and the primers used to amplify and sequence the PYD and NACHT domain are shown in Supplementary Table 2. The sequences were analyzed and assembled using both Sequencher™ 3.1 (Gene Codes) and MacVector™ 6.5.1 (Oxford Molecular).

2.9. Primate and mouse ortholog alignment and analysis

DNA and predicted protein sequences were aligned using ClustalW and modified by visual inspection (Thompson et al., 1994). MacClade was used to trace amino acids along a total evidence phylogram (Goodman et al., 1998; Murphy et al., 2001) and to infer the most closely matched ancestral states (Maddison and Maddison, 1989). A total of 21 amino acids, where known human mutations have been described, were analyzed. Maximum Likelihood Analysis was performed using a total evidence tree representing the relationships of the primates in this data set (Goodman et al., 1998). Positive selection was assessed using the ratio of non-synonymous substitutions per nonsynonymous site (d_N) to synonymous substitutions per synonymous site (d_S). The codon-based likelihood method was used to analyze lineage specific d_N/d_S ratios (Schaner et al., 2001; Yang, 1998). We used the program PAML to apply two models of nucleotide sequence evolution to our data set, the "free ratio" model and the "simple" model (Yang, 1998). In theory, a d_N/d_S ratio equal to 1.0 indicates neutral change, a d_N/d_S ratio less than 1.0 indicates purifying selection, and a d_N/d_S ratio greater than 1.0 indicates positive selection (Schaner et al., 2001).

Analysis of orthology relationships among mouse and human NALP homologs was carried out by combining a phylogenetic reconstruction of the gene family with a genomic synteny comparison of mouse and human chromosomes. Predicted genes from the Ensembl mouse and human builds 32 and 34 (http://www.ensembl.org/), respectively (Feb. 2004) were used to construct a gene family alignment with and modified by visual inspection (Thompson et al., 1994). Bootstrapped neighbor joining and maximum parsimony phylogenies were calculated using Phylip 3.6 (Felsenstein, 2000). Maximum likelihood branch lengths were calculated based on the parsimony topology using Tree-Puzzle (Schmidt et al., 2002). Mouse–human synteny blocks (regions of genomic homology) were identified in chromosomes M7/H19, M7/H11, and M11/H1 using DiagHunter (Cannon et al., 2003). Orthologous and paralogous genes were confirmed using OrthoParaMap by combining synteny predictions and gene family phylogeny, with methods and parameters previously described (Cannon and Young, 2003).

3. Results and discussion

3.1. Analysis of mouse CIAS1 and other genes in the NALP family

When the *hCIAS1*-predicted protein sequence (aaL33908) was used as a query sequence on NCBI's Standard protein–protein BLAST (blastp) program, the resultant matches included *hCIAS1* (*NALP3*) and the other 13 human NALP genes (Tschopp et al., 2003). We found the chromosomal location for all 14 known human NALP genes using the LocusLink button

(Table 1). *hCIAS1* is unique in its localization to 1q44, because most of the other human NALP genes cluster on Chr 11 and 19, except for *NALP1*, which is localized to Chr 17. NCBI's HomoloGene link identified mouse orthologs to 10 of 14 human NALP genes; however, orthologs for *NALP 7, 8, 11*, and *13* were not identified. *mCIAS1* is located on a 23-kb region on Chr 11B1.3, a region that has limited synteny to human Chr 1q44. All of the other mouse NALP genes cluster on Chr 7 except for *NALP1*, which is located at Chr 11B4. This clustering suggests gene duplications (Harton et al., 2002), and the additional human NALP genes on Chr 19 not found in the mouse indicate further gene duplications. Combining phylogenetic and comparative synteny information using DiagHunter (Cannon et al., 2003) and OrthoParaMap (Cannon and Young, 2003) indicates local gene duplications of human NALP 2 and 7 on chromosome 19 following speciation, local duplication of mouse NALP 9a and 9c following speciation, and probable loss of several mouse orthologs (Fig. 1). The presence of *hCIAS1* at the telomere on human Chr 1q in a region with limited synteny to mouse Chr 11B1.3 may suggest substantial rearrangements in the mouse and/or human chromosomes in these regions during mammalian evolution. However, high levels of conservation in the coding sequence of *hCIAS1* and *mCIAS1* (NALP3) suggest that these are genuinely orthologs (Fig. 1).

We independently confirmed the exon structure of *mCIAS1* by sequencing all nine exons and splice junctions in three commonly studied inbred strains of mice. From these sequences, we discovered only one variation (T to C) at a nucleotide that is 27 bp beyond the intron 4–exon 4 junction. All other exons and available surrounding intron sequences were completely conserved in all three strains. The mouse exon structure bears very close resemblance to the human exon structure (Supplementry Fig. 1). Comparison of the complete mouse and human ORF shows they have an 80.8% identity. This is different from *MEFV*, the gene that codes for pyrin, which shows only a 65.8% identity between mouse and human (Chae et al., 2000), suggesting different evolutionary pressures on these two related genes.

The *mCIAS1* gene has nine coding exons with a putative initiator methionine codon in good agreement with the Kozak criteria and a stop codon in the final exon. Cloning and sequencing of the cDNA and comparison to the genomic sequence confirmed the assignment of the donor and acceptor splice sites of the exon–intron boundaries. 5′ RACE of *mCIAS1* identified two untranslated exons and alternative splicing, which results in two transcriptional start sites. One isoform contains two untranslated exons of 19 bp and 59 bp, respectively. The second isoform consists of one large (226 bp) untranslated exon. This pattern differs from *hCIAS1*, where only one transcriptional start site was identified and no additional untranslated 5′ exons were identified. 3′ RACE demonstrated approximately 700 untranslated bp before the poly A tail consistent with AF486632 (Kikuchi-Yanoshita et al., 2003). We also detected alternative splicing of *mCIAS1* exons 4–9 from mouse peripheral blood leukocyte cDNA. Alternative splicing in this region has also been described in bone marrow-derived mast cells (Kikuchi-Yanoshita et al., 2003). The finding of alternative splicing in this region correlates with *hCIAS1*, where extensive alternative splicing was apparent in this region of cDNA from human peripheral blood leukocytes (Hoffman et al., 2001a).

The *mCIAS1* ORF encodes a putative 1033-aa protein with a predicted size of 118.3 kDa and a *p*I of 6.55. As in *hCIAS1*, the first coding exon is predicted to code for a PYD; the large central exon is predicted to code for a NACHT domain and each of the 171 bp exons code for two leucine-rich repeats, while the final coding exon codes for one leucine-rich repeat (Supplementry Fig. 1). The predicted amino acid sequence has an 82.7% identity and an 89.6% similarity between human and mouse. This is different from the related protein pyrin, another PYD containing protein, which only has a 47.6% identity and a 65.5% similarity between human and mouse homologs (Chae et al., 2000). The PYD of *CIAS1* shows the greatest homology with 93.0% identity/97.2% similarity. The NACHT domain shows 85.0% identity/91.2% similarity, and the LRR region shows an 83.6% identity/90.5% similarity. The alignments of the NACHT and PYDs are shown in Figs. 2 and 3. A total of 21 amino acids are shown where human mutations have been identified. With the exception of aa198 and aa662, all amino acids where human disease causing mutations occur are conserved in the mouse. In the mouse, aa196 (corresponding to human aa198) is a methionine. This is the mutated aa (V198M) observed in some patients with FCAS and MWS (Aganna et al., 2002; Hoffman et al., 2001a). Additionally, valine is substituted for a methionine at position aa662 in the mouse. In humans, M662T has been identified in a patient with NOMID (Feldmann et al., 2002). Interestingly, the V198M mutation has been seen in up to 6% of normal Caucasian controls (unpublished data), suggesting that it is either not a fully penetrant mutation or it is simply a polymorphism. The conservation of these amino acids throughout mammalian evolution is expected if one assumes that they are important for protein function. However, once again, this is very different from the case of pyrin where only 1 of 10 amino acids, where human mutations have been identified, is conserved (Schaner et al., 2001).

3.2. Expression analysis and tissue distribution

Northern blot analyses of human tissues identified expression in peripheral blood leukocytes and no significant expression in other tissues. Northern analysis in mouse tissues identified a single transcript expressed at low levels in liver; no expression was detectable in other tissues (data not shown). This transcript, approximately 4.0 kb, is similar in size to *hCIAS1* cDNA and is consistent with the longest complete *mCIAS1* cDNA identified. Because there is limited representation of mouse tissue on available Northern blots (eye, skin, and PBMCs were not included on the Northern blots), we performed Taqman® quantitative real-time PCR, which identified prominent expression of *mCIAS1* in skin and eye (Fig. 4A). This finding is in strong agreement with human disease phenotypes in that rash is present in all patients with *CIAS1* mutations, conjunctivitis is commonly seen in FCAS and MWS (Hoffman et al., 2001b). Low level expression of *mCIAS1* was detected in liver in agreement with Northern analysis. The relative higher expression of CIAS1 in liver compared to other tissues on the blot may be due to contaminating peripheral blood leukocytes.

Significant expression of *mCIAS1* was detected in peripheral blood leukocytes by quantitative real-time PCR similar to the expression pattern in *hCIAS1* (Fig. 4B). Quantitative real-time PCR of leukocyte subpopulations showed significantly higher relative expression of *mCIAS1* in granulocyte and monocyte fractions, with relatively less expression in bone marrow-derived mast cells, and low expression in lymphocyte fractions. This

cellular expression pattern is similar to that of *hCIAS1* (Manji et al., 2002), as well as human *NOD2* (Ogura et al., 2001b) and human *pyrin* (Tidow et al., 2000), and is consistent with the role of these proteins in innate immunity. Additionally, granulocytes are elevated in peripheral blood and are visualized in biopsies from affected skin in patients with *CIAS1* mutations.

3.3. Evolutionary analysis

All of the new and old world primates (including human) shared significant homology in the NACHT domain, with the DNA identities all greater than 87%, and the amino acid identities and similarities all greater than 90% and 93%, respectively. Fig. 2 shows an alignment of the predicted amino acid composition of the NACHT domain in representative primates. Old and new world primates not shown in Table 2 show very similar results to those of their corresponding orders. The amino acid positions, where human disease mutations have been identified, are conserved within the primates we sequenced and the mouse with differences in only three aa. At aa198, the baboon is heterozygous (valine or isoleucine), and the mouse is homozygous for methionine; at aa374, the common marmoset has a threonine instead of an alanine; and at aa662, all of the primates sequenced, and the mouse have a valine instead of a methionine.

The DNA from the lower primates and mammals was more difficult to amplify and sequence, therefore some of the NACHT domains were not completely sequenced in these animals. As in the higher mammals, the sequence obtained still showed significant similarities (Table 2), and the amino acids where human disease causing mutations occur were conserved. In an attempt to delineate the evolutionary age of *CIAS1*, we also tried to amplify and sequence select birds and reptiles, but were unable to confirm any orthologs in these proposed mammalian predecessors. However, we were able to identify a possible ortholog for *CIAS1* in the database for the vertabrate puffer-fish, *F. rubripes* (SINFRUG00000i50262), but not in the zebrafish (http://www.ensembl.org/).

Recently, an evolutionary analysis of mutations in pyrin, another PYD-containing protein, demonstrated that 7 of 10 FMF causing mutations in one domain are present in many of the wild-type primates (Schaner et al., 2001). A similar analysis of 21 mutations (all with frequencies < .00001 in the general population) within *CIAS1* (INFEVERS: http://fmf.igh.cnrs.fr/infevers) indicates that none of these mutations (except V198M) are present in primates; in fact, the vast majority of them represent the only amino acid change evident during the evolutionary history of that site. In contrast to pyrin, the evolutionary history of Cryopyrin mutations suggests that the wild-type amino acids have been strongly selected for. In our analysis, the data fit the “free ratio” model with high significance ($P \ll 0.001$). This model posits that d_N/d_S ratios vary along each branch of the phylogram. The highest rate ratio of nonsynonymous to synonymous substitutions that we obtained using this model was 0.26, and the rest of the values were much lower. These data strongly suggest that Cryopyrin has been under purifying selection throughout its evolution.

The evolutionary history of pyrin and Cryopyrin may point to fundamental differences in function and/or position within inflammatory pathways. While pyrin and Cryopyrin appear to be involved in the activation of caspase 1 and NF-κB through their interactions with

Apoptosis-associated speck like protein (ASC; Manji et al., 2002; Richards et al., 2001; Srinivasula et al., 2002), it has been proposed that pyrin has an inhibitory role and Cryopyrin has an activating role (Dowds et al., 2003). Although pyrin and Cryopyrin share a similar N-terminal domain (PYD), the rest of the pyrin protein structure is unique among PYD-containing proteins, while the C-terminal region of the Cryopyrin protein is homologous to the large family of NALP proteins (Tschopp et al., 2003). It is also of note that FMF is typically recessive, while FCAS is transmitted in an autosomal dominant fashion. It has been suggested that pyrin may be responding to positive selective pressure, and disease may be the homozygous manifestation of an advantageous heterozygous state (International FMF Consortium, 1997). In contrast, heterozygous mutations in the strongly purified NACHT domain of Cryopyrin may alter function resulting in disease.

3.4. Conclusions

The highly conserved nature of Cryopyrin throughout mammalian evolution and expression in inflammatory cells supports its proposed crucial role in innate immune function. An important regulatory function for Cryopyrin is further supported by the fact that single heterozygous missense mutations in *hCIAS1* in areas of highly conserved amino acids of Cryopyrin cause a variety of inflammatory phenotypes ranging from cold sensitivity to severe multi-system involvement.

Supplementary Material

Refer to Web version on PubMed Central for supplementary material.

Acknowledgments

The authors wish to thank Jyothi Nayar and Antonia Boyer for general technical assistance, John Weger, Stefanie Ness, and Dena Cassel for DNA sequencing assistance, Sherry Soefje and Olaina Anderson for editorial advice, and Richard Kolodner, Bill Biggs, Deborah Gumucio, Gary Firestein, Gregg Silverman, and Oliver Ryder for helpful advice. Primate DNA was obtained from Deborah Gumucio and other mammalian DNA samples were obtained from the Center for the Reproduction of Endangered Species. This work was supported by the Rheumatic Diseases Core Center, the Ludwig Institute of Cancer Research, and NIH NIAID RO1 AI 52430.

Abbreviations

hCIAS1	human *CIAS1*
PYD	pyrin domains
LRR	leucine-rich repeat
MHC	major histocompatibility complex
CIITA	class II transactivator
FMF	familial Mediterranean fever
FCAS	familial cold autoinflammatory syndrome
MWS	Muckle– Wells syndrome
NOMID	neonatal onset multisystem inflammatory disease

DNA	deoxyribonucleic acid
RNA	ribonucleic acid
NCBI	National Center for Biotechnology Information
aa	amino acid
mCIAS1	mouse *CIAS1*
Chr	chromosome
PCR	polymerase chain reaction
cDNA	complementary DNA
PBMC	peripheral blood mononuclear cells
REU	relative expression units
ASC	apoptotic speck protein
RACE	rapid amplification of cDNA ends
ORF	open reading frame
bp	base pair
kb	kilo-base
kDa	kilo-Dalton

References

Aganna E, Martinon F, Hawkins PN, Ross JB, Swan DC, Booth DR, Lachmann HJ, Bybee A, Gaudet R, Woo P, Feighery C, Cotter FE, Thome M, Hitman GA, Tschopp J, McDermott MF. Association of mutations in the NALP3/CIAS1/PYPAF1 gene with a broad phenotype including recurrent fever, cold sensitivity, sensorineural deafness, and AA amyloidosis. Arthritis Rheum. 2002; 46:2445–2452. [PubMed: 12355493]

Boyle DL, Rosengren S, Kavanaugh A, Bugbee W, Firestein GS. Quantitative biomarker analysis of synovial gene expression by real-time PCR. Arthritis Res Ther. 2003; 5:R352–R360. [PubMed: 14680510]

Cannon SB, Young ND. OrthoParaMap: distinguishing orthologs from paralogs by integrating comparative genome data and gene phylogenies. BMC Bioinformatics. 2003; 4:35. [PubMed: 12952558]

Cannon SB, Kozik A, Chan B, Michelmore R, Young ND. DiagHunter and GenoPix2D: programs for genomic comparisons, large-scale synteny-discovery, and visualization. Genome Biol. 2003; 4:R68. [PubMed: 14519203]

Chae JJ, Centola M, Aksentijevich I, Dutra A, Tran M, Wood G, Nagaraju K, Kingma DW, Liu PP, Kastner DL. Isolation, genomic organization, and expression analysis of the mouse and rat homologs of MEFV, the gene for familial Mediterranean fever. Mamm Genome. 2000; 11:428–435. [PubMed: 10818206]

Chae JJ, Komarow HD, Cheng J, Wood G, Raben N, Liu PP, Kastner DL. Targeted disruption of pyrin, the FMF protein, causes heightened sensitivity to endotoxin and a defect in macrophage apoptosis. Mol Cell. 2003; 11:591–604. [PubMed: 12667444]

Chang CH, Guerder S, Hong SC, van Ewijk W, Flavell RA. Mice lacking the MHC class II transactivator (CIITA) show tissue-specific impairment of MHC class II expression. Immunity. 1996; 4:167–178. [PubMed: 8624807]

Dode C, Le Du N, Cuisset L, Letourneur F, Berthelot JM, Vaudour G, Meyrier A, Watts RA, Scott DG, Nicholls A, Granel B, Frances C, Garcier F, Edery P, Boulinguez S, Domergues JP, Delpech M, Grateau G. New mutations of CIAS1 that are responsible for Muckle– Wells syndrome and familial cold urticaria: a novel mutation underlies both syndromes. Am J Hum Genet. 2002; 70:1498–1506. [PubMed: 11992256]

Dowds TA, Masumoto J, Chen FF, Ogura Y, Inohara N, Nunez G. Regulation of Cryopyrin/Pypaf1 signaling by pyrin, the familial Mediterranean fever gene product. Biochem Biophys Res Commun. 2003; 302:575–580. [PubMed: 12615073]

Feldmann J, Prieur AM, Quartier P, Berquin P, Certain S, Cortis E, Teillac-Hamel D, Fischer A, Basile Gd Gde S. Chronic infantile neurological cutaneous and articular syndrome is caused by mutations in CIAS1, a gene highly expressed in polymorphonuclear cells and chondrocytes. Am J Hum Genet. 2002; 71:198–203. [PubMed: 12032915]

Felsenstein, J. Distributed by the author. Department of Genetics, University of Washington; Seattle: 2000. PHYLIP (Phylogeny Inference Package) version 3.6.

French FMF Consortium. A candidate gene for familial Mediterranean fever. The French FMF Consortium. Nat Genet. 1997; 17:25–31. [PubMed: 9288094]

Goodman M, Porter CA, Czelusniak J, Page SL, Schneider H, Shoshani J, Gunnell G, Groves CP. Toward a phylogenetic classification of primates based on DNA evidence complemented by fossil evidence. Mol Phylogenet Evol. 1998; 9:585–598. [PubMed: 9668008]

Harton JA, Linhoff MW, Zhang J, Ting JP. Cutting edge: CATERPILLER: a large family of mammalian genes containing CARD, pyrin, nucleotide-binding, and leucine-rich repeat domains. J Immunol. 2002; 169:4088–4093. [PubMed: 12370334]

Hoffman HM, Mueller JL, Broide DH, Wanderer AA, Kolodner RD. Mutation of a new gene encoding a putative pyrin-like protein cause familial cold autoinflammatory syndrome and Muckle–Wells syndrome. Nat Genet. 2001a; 29:301–305. [PubMed: 11687797]

Hoffman HM, Wanderer AA, Broide DH. Familial cold auto-inflammatory syndrome: phenotype and genotype of an autosomal dominant periodic fever. J Allergy Clin Immunol. 2001b; 108:615–620. [PubMed: 11590390]

Hugot JP, Chamaillard M, Zouali H, Lesage S, Cezard JP, Belaiche J, Almer S, Tysk C, O'Morain CA, Gassull M, Binder V, Finkel Y, Cortot A, Modigliani R, Laurent-Puig P, Gower-Rousseau C, Macry J, Colombel JF, Sahbatou M, Thomas G. Association of NOD2 leucine-rich repeat variants with susceptibility to Crohn's disease. Nature. 2001; 411:599–603. [PubMed: 11385576]

International FMF Consortium. Ancient missense mutations in a new member of the RoRet gene family are likely to cause familial Mediterranean fever. The International FMF Consortium. Cell. 1997; 90:797–807. [PubMed: 9288758]

Kikuchi-Yanoshita R, Taketomi Y, Koga K, Sugiki T, Atsumi Y, Saito T, Ishii S, Hisada M, Suzuki-Nishimura T, Uchida MK, Moon TC, Chang HW, Sawada M, Inagaki N, Nagai H, Murakami M, Kudo I. Induction of Pypaf1 during in vitro maturation of mouse mast cells. J Biochem (Tokyo). 2003; 134:699–709. [PubMed: 14688236]

Kolodner RD, Tytell JD, Schmeits JL, Kane MF, Gupta RD, Weger J, Wahlberg S, Fox EA, Peel D, Ziogas A, Garber JE, Syngal S, Anton-Culver H, Li FP. Germ-line msh6 mutations in colorectal cancer families. Cancer Res. 1999; 59:5068–5074. [PubMed: 10537275]

Maddison WP, Maddison DR. Interactive analysis of phylogeny and character evolution using the computer program MacClade. Folia Primatol (Basel). 1989; 53:190–202. [PubMed: 2606395]

Manji GA, Wang L, Geddes BJ, Brown M, Merriam S, Al-Garawi A, Mak S, Lora JM, Briskin M, Jurman M, Cao J, DiStefano PS, Bertin J. PYPAF1: a PYRIN-containing Apaf1-like protein that assembles with ASC and regulates activation of NF-kB. J Biol Chem. 2002; 277:11570–11575. [PubMed: 11786556]

Miceli-Richard C, Lesage S, Rybojad M, Prieur AM, Manouvrier-Hanu S, Hafner R, Chamaillard M, Zouali H, Thomas G, Hugot JP. CARD15 mutations in Blau syndrome. Nat Genet. 2001; 29:19–20. [PubMed: 11528384]

Muckle TJ. The 'Muckle– Wells' syndrome. Br J Dermatol. 1979; 100:87–92. [PubMed: 427013]

Murphy WJ, Eizirik E, O'Brien SJ, Madsen O, Scally M, Douady CJ, Teeling E, Ryder OA, Stanhope MJ, de Jong WW, Springer MS. Resolution of the early placental mammal radiation using Bayesian phylogenetics. Science. 2001; 294:2348–2351. [PubMed: 11743200]

Neven B, Callebaut I, Prieur AM, Feldmann J, Bodemer C, Lepore L, Derfalvi B, Benjaponpitak S, Vesely R, Sauvain MJ, Oertle S, Allen R, Morgan G, Borkhardt A, Hill C, Gardner-Medwin J, Fischer A, De Saint Basile G. Molecular basis of the spectral expression of CIAS1 mutations associated with phagocytic cell-mediated auto-inflammatory disorders (CINCA/NOMID, MWS, FCU). Blood. 2004; 103:2809–2815. [PubMed: 14630794]

Ogura Y, Bonen DK, Inohara N, Nicolae DL, Chen FF, Ramos R, Britton H, Moran T, Karaliuskas R, Duerr RH, Achkar JP, Brant SR, Bayless TM, Kirschner BS, Hanauer SB, Nunez G, Cho JH. A frameshift mutation in NOD2 associated with susceptibility to Crohn's disease. Nature. 2001a; 411:603–606. [PubMed: 11385577]

Ogura Y, Inohara N, Benito A, Chen FF, Yamaoka S, Nunez G. Nod2, a Nod1/Apaf-1 family member that is restricted to monocytes and activates NF-kappaB. J Biol Chem. 2001b; 276:4812–4818. [PubMed: 11087742]

Prieur AM, Griscelli C, Lampert F, Truckenbrodt H, Guggenheim MA, Lovell DJ, Pelkonnen P, Chevrant-Breton J, Ansell BM. A chronic, infantile, neurological, cutaneous and articular (CINCA) syndrome. A specific entity analysed in 30 patients. Scand J Rheumatol. 1987; (Suppl 66):57–68.

Razin E, Cordon-Cardo C, Good RA. Growth of a pure population of mouse mast cells in vitro with conditioned medium derived from concanavalin A-stimulated splenocytes. Proc Natl Acad Sci U S A. 1981; 78:2559–2561. [PubMed: 6166010]

Reed JC, Doctor K, Rojas A, Zapata JM, Stehlik C, Fiorentino L, Damiano J, Roth W, Matsuzawa S, Newman R, Takayama S, Marusawa H, Xu F, Salvesen G, Godzik A. Comparative analysis of apoptosis and inflammation genes of mice and humans. Genome Res. 2003; 13:1376–1388. [PubMed: 12819136]

Richards N, Schaner P, Diaz A, Stuckey J, Shelden E, Wadhwa A, Gumucio DL. Interaction between pyrin and the apoptotic speck protein (ASC) modulates ASC-induced apoptosis. J Biol Chem. 2001; 9:9.

Schaner P, Richards N, Wadhwa A, Aksentijevich I, Kastner D, Tucker P, Gumucio D. Episodic evolution of pyrin in primates: human mutations recapitulate ancestral amino acid states. Nat Genet. 2001; 27:318–321. [PubMed: 11242116]

Schmidt HA, Strimmer K, Vingron M, von Haeseler A. TREE-PUZZLE: maximum likelihood phylogenetic analysis using quartets and parallel computing. Bioinformatics. 2002; 18:502–504. [PubMed: 11934758]

Srinivasula SM, Poyet JL, Razmara M, Datta P, Zhang Z, Alnemri ES. The PYRIN-CARD protein ASC is an activating adaptor for caspase-1. J Biol Chem. 2002; 277:21119–21122. [PubMed: 11967258]

Steimle V, Otten LA, Zufferey M, Mach B. Complementation cloning of an MHC class II transactivator mutated in hereditary MHC class II deficiency (or bare lymphocyte syndrome). Cell. 1993; 75:135–146. [PubMed: 8402893]

Thompson JD, Higgins DG, Gibson TJ. CLUSTAL W: improving the sensitivity of progressive multiple sequence alignment through sequence weighting, position-specific gap penalties and weight matrix choice. Nucleic Acids Res. 1994; 22:4673–4680. [PubMed: 7984417]

Tidow N, Chen X, Muller C, Kawano S, Gombart AF, Fischel-Ghodsian N, Koeffler HP. Hematopoietic-specific expression of MEFV, the gene mutated in familial Mediterranean fever, and sub-cellular localization of its corresponding protein, pyrin. Blood. 2000; 95:1451–1455. [PubMed: 10666224]

Tschopp J, Martinon F, Burns K. NALPs: a novel protein family involved in inflammation. Nat Rev, Mol Cell Biol. 2003; 4:95–104. [PubMed: 12563287]

Yang Z. Likelihood ratio tests for detecting positive selection and application to primate lysozyme evolution. Mol Biol Evol. 1998; 15:568–573. [PubMed: 9580986]

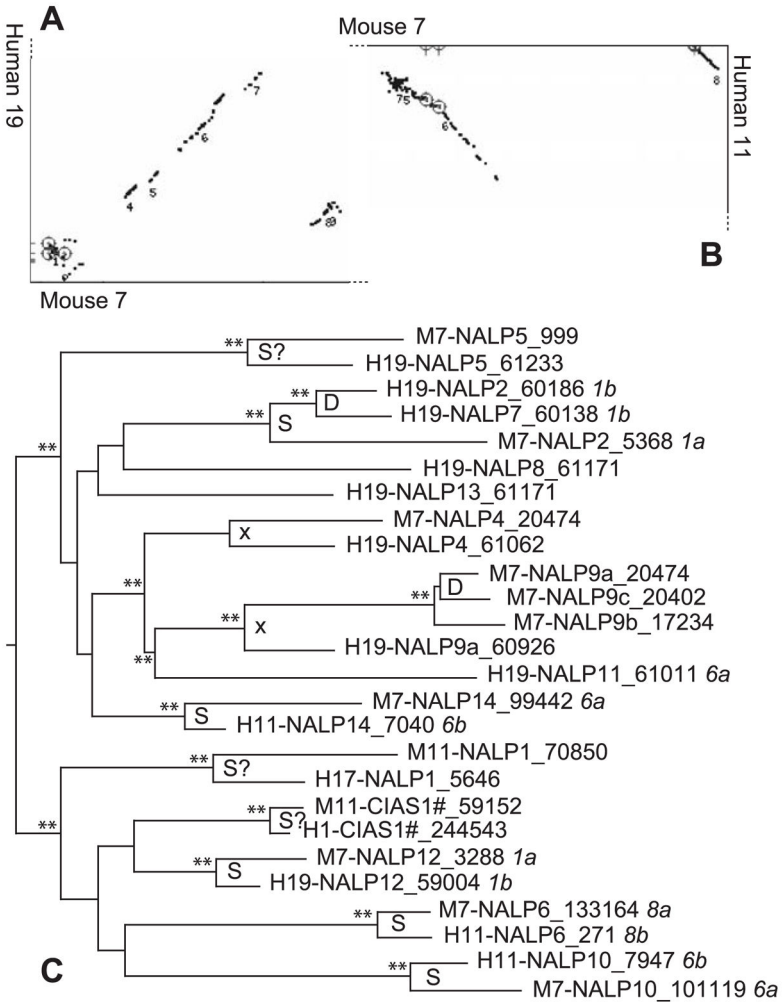

Fig. 1.

The human and mouse NALP gene phylogeny and genomic context. Dot plots show regions of mouse– human synteny (diagonal lines) near NALP-containing regions (synteny blocks are labeled with consecutive numbers as assigned by the program) in (A) human 19/mouse 7 and (B) human 11/mouse 7. The locations of NALP genes are shown with short lines on the axes. Where two of these genes from mouse and human intersect with a diagonal, they are highlighted with bulls-eyes. These points represent candidate orthologs. The phylogeny (C) shows human (Hs) and mouse (Mm) genes, genomic positions (gene midpoints in kb), and corresponding synteny blocks labeled with italic numbers (*a*, mouse; *b*, human). Gene duplications clearly originating in speciation-derived synteny blocks are indicated with S, gene duplications likely to be orthologs but without strong supporting synteny information are indicated with 'S?', and those arising through local gene duplications following speciation are indicated with D. Nodes marked with "x" likely originated through speciation (they are the reciprocal best matches between mouse and human), although no synteny is detectable. # CIAS1 is also known as NALP3.

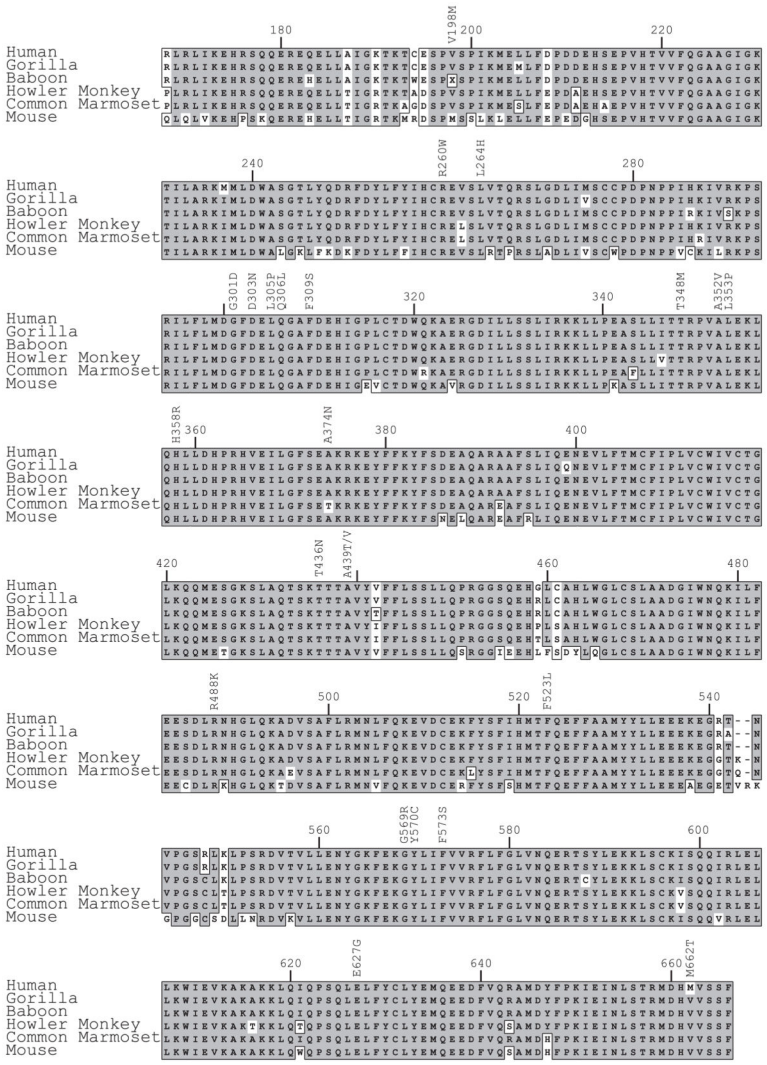

Fig. 2.

Cryopyrin NACHT domain aa alignment. The amino acid sequences shown are from the NACHT domain (Human aa168 to aa666 and Mouse aa166 to aa668). *G. gorilla* (gorilla) is shown as a close relative to *H. sapiens* (human), *T. gelada* (baboon) is an old world primate, while *A. belzebul* (howler monkey) and *C. jacchus* (common marmoset) are different ends of the new world primate infraorder. The shaded regions are exact matches, while nonshaded regions are similar amino acids. Separated boxed amino acids are dissimilar. The X located at aa198 for the baboon indicates heterozygosity at this base pair. The predicted amino acids are either a valine or isoleucine.

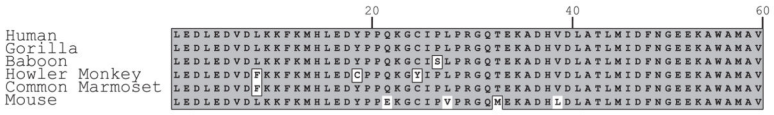

Fig. 3.

Cryopyrin pyrin domain aa alignment. The amino acid sequence shown is the first 60 amino acids of the pyrin domain (73 aa). The shaded regions are exact matches, while nonshaded regions are similar amino acids. Separated boxed amino acids are dissimilar.

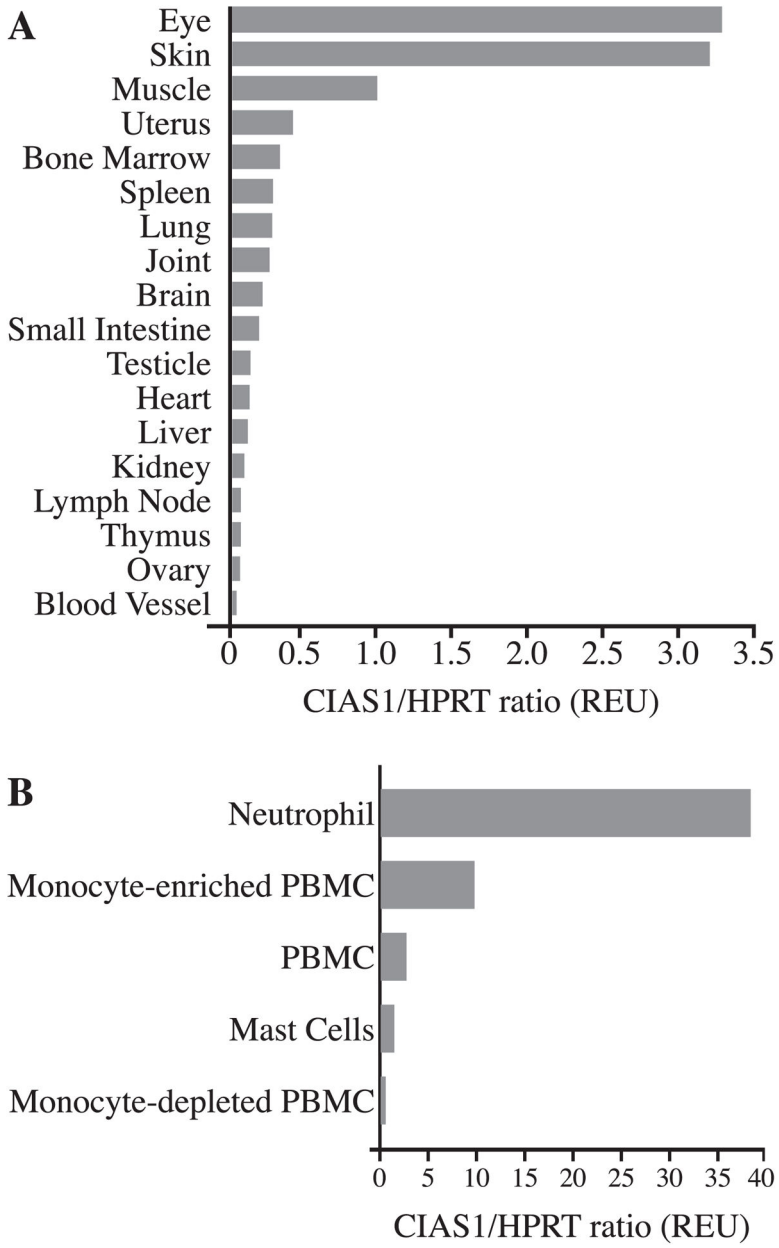

Fig. 4.

Expression analysis of mouse *CIAS1*. (A) *mCIAS1* mRNA levels assayed from tissues and normalized to those of *HPRT* mRNA. (B) *mCIAS1* mRNA levels assayed from leukocyte fractions and normalized to those of *HPRT* mRNA.

Table 1

Human and mouse NALP genes

NALP	Human Ensembl gene[a]	Locus link[a]	Human chromosome	Mouse ensembl gene[a]	Locus link[a]	Mouse chromosome	% aa identity
1	ENSG00000091592	22861	17p13	ENSMUSG00000051983	195046	11B4	78.2
2	ENSG00000022556	55655	19q13.42	ENSMUSG00000035177	232827	7A1	73.1
CIAS1[a]	ENSG00000162711	114548	1q44	ENSMUSG00000032691	216799	11B1.3	82.7
4	ENSG00000160505	147945	19q13.43	ENSMUSG00000040601	270522	7A3	72.2
5	ENSG00000171487	126206	19q13.43	ENSMUSG00000015721	23968	7A2	77.0
6	ENSG00000174885	171389	11p15	ENSMUSG00000038745	101613	7F4	78.3
7	ENSG00000167634	199713	19q13.42	–	–	–	–
8	ENSG00000179709	126205	19q13.43	–	–	–	–
9a	ENSG00000185792	338321	19q13.43	ENSMUSG00000040601	233001	7A3	74.6
9b	–	–	–	ENSMUSG00000054102	243874	7 21.1	–
9c	–	–	–	ENSMUSG00000040614	330490	7A3	–
10	ENSG00000182261	338322	11p15.4	ENSMUSG00000049709	244202	7 E3	80.8
11	ENSG00000179873	204801	19q13.43	–	–	–	–
12	ENSG00000142405	91662	19q13.42	ENSMUSG00000054891	378425	7A1	79.5
13	ENSG00000173572	126204	19q13.43	–	–	–	–
14	ENSG00000158077	338323	11p15.4	ENSMUSG00000016626	381907	7 E3	76.7

[a]Also known as NALP3.

Table 2

NACHT domain identity and similarities in mammalian CIAS1 orthologs

Species	DNA[a]	aa[b]	# Of bp[c]
Mouse	82.0	85.0/91.2	1503
Gorilla	98.7	98.6/99.8	1497
Baboon	97.5	98.0/99.0	1497
Howler monkey	92.9	95.6/98.2	1500
Common marmoset	92.4	94.2/97.4	1500
Dwarf lemur	90.4	91.9/94.5	1365
Tarsier	84.7	88.6/92.0	1311
Armadillo	84.3	90.3/94.4	1239
African elephant	85.3	89.6/93.2	1239
Hedgehog	80.7	83.9/91.2	1110

[a]Percentage identity.

[b]Percentage identity/percentage similarity.

[c]Number of base pairs sequenced for each animal.